Thallium as a Tracer for Preindustrial Volcanic Eruptions in an Ice Core Record from Illimani, Bolivia

7 AUTHORS, INCLUDING:

Thomas Kellerhals
Universität Bern
8 PUBLICATIONS **137** CITATIONS

SEE PROFILE

L. Wacker
ETH Zurich
154 PUBLICATIONS **2,467** CITATIONS

SEE PROFILE

Heinz Gaeggeler
Paul Scherrer Institut
298 PUBLICATIONS **6,586** CITATIONS

SEE PROFILE

Margit Schwikowski
Paul Scherrer Institut
183 PUBLICATIONS **3,069** CITATIONS

SEE PROFILE

Thallium as a Tracer for Preindustrial Volcanic Eruptions in an Ice Core Record from Illimani, Bolivia

THOMAS KELLERHALS,*,†,‡
LEONHARD TOBLER,‡ SABINA BRÜTSCH,‡
MICHAEL SIGL,†,‡ LUKAS WACKER,§
HEINZ W. GÄGGELER,†,‡ AND
MARGIT SCHWIKOWSKI‡,∥

Department of Chemistry and Biochemistry, University of Bern, Switzerland, Paul Scherrer Institut, Villigen, Switzerland, Institute for Particle Physics, ETH Zürich, Switzerland, and Oeschger Centre for Climate Change Research, University of Bern, Switzerland

Trace element records from glacier and ice sheet archives provide insights into biogeochemical cycles, atmospheric circulation changes, and anthropogenic pollution history. We present the first continuous high-resolution thallium (Tl) record, derived from an accurately dated ice core from tropical South America, and discuss Tl as a tracer for volcanic eruptions. We identify four prominent Tl peaks and propose that they represent signals from the massive explosive eruptions of the "unknown 1258" A.D. volcano, of Kuwae (~1450 A.D.), Tambora (1815 A.D.), and Krakatoa (1883 A.D.). The highly resolved record was obtained with an improved setup for the continuous analysis of trace elements in ice with inductively coupled plasma sector field mass spectrometry (ICP-SFMS). The new setup allowed for a stronger initial acidification of the meltwater and shorter tubing length, thereby reducing the risk of memory effects and losses of analytes to the capillary walls. With a comparison of the continuous method to the established conventional decontamination and analysis procedure for discrete samples, we demonstrate the accuracy of the continuous method for Tl analyses.

Introduction

Most investigations on heavy metals in snow and ice were focused until recently on the contribution of anthropogenic activities to the measured concentrations of a wide range of metals [1–3]. A few studies also aimed at a characterization of the natural trace metal emissions to the atmosphere, using their deposition histories archived in glaciers and ice sheets [4, 5]. Especially for preindustrial time periods when anthropogenic emissions are not the dominant source, trace metals have a great potential as atmospheric tracers for geochemical cycles. For a suite of trace elements, volcanic emissions are an important source term [6, 7]. Bi, for instance,

was suggested as a tracer for volcanic emissions because its other sources are thought to be very limited [8]. Together with Bi, Pb, Cu, Zn, and a large suite of other metals, Tl was measured in plumes from the Kilauea volcano, where it occurred in similar proportions as Pb [7].

As a natural constituent of the Earth's crust, Tl is a widely spread element. However, the low crustal abundance of Tl (approximately 0.52 mg kg^{-1} in the Earth's continental crust [9]) makes it difficult to track its geochemical cycle. Today, coal combustion and smelting activities are the main anthropogenic sources for Tl emissions to the atmosphere [10, 11]. Source attribution for preindustrial time periods (e.g., volcanic emissions, continental dust, early smelting activities, and wildfires) is very difficult due to the paucity of available data. Although Tl is a highly toxic element, there are much fewer studies on Tl than on other toxic elements such as Pb, Cd, or Hg. This is at least partly due to the extremely low concentrations of Tl in environmental samples, necessitating rigorous decontamination procedures and highly sensitive analytical methods. Over the years, ICP-SFMS has proved to represent one of the most sensitive approaches for the determination of trace elements in the environment.

To date, there are only few studies reporting on Tl concentrations in snow samples and ice cores [12–14]. A first long-term deposition record of Tl in central Europe was derived from a Swiss peat bog [15]. The constant Tl to Sc ratio during the preindustrial time period (~14 500 years before present (B.P.) to 1840 A.D.) showed that atmospheric soil dust was the dominant source of Tl input [15]. Conversely, a Tl record from the Devon Island ice cap was interpreted as evidence for early anthropogenic contributions from mining activities [13]. However, both of these Tl records are by far not resolved highly enough to allow for the identification of potential short-term inputs from for example explosive volcanic eruptions.

Here, we present the first continuous long-term high-resolution Tl record, derived from a high-altitude ice core from Nevado Illimani in the eastern Bolivian Andes. We identify a Tl signal from massive explosive volcanic eruptions that occurs in the ice core together with commonly used volcanic eruption tracers like excess sulfate ($exSO_4^{2-}$) and fluoride (F^-). The time period discussed in this study covers the last 2000 years, not including the firn part of the core (1964 A.D. to 1999 A.D.), where no trace element analysis was performed. The high-resolution Tl record was obtained with an improved setup for the continuous analysis of trace elements in ice with ICP-SFMS. The use of a melter head (MH) for the ice core decontamination speeded up the labor-intensive conventional decontamination procedure, reduced the risk of sample contamination, and increased the achievable sample resolution [16, 17]. To illustrate the accuracy of the continuous method for the analysis of Tl in ice, we compare it to a well established method that consists in analyzing thoroughly decontaminated discrete samples [18–20].

Materials and Methods

Ice Cores. Two parallel ice cores were retrieved from a glacier saddle on Nevado Illimani (16°37′S, 67°46′W, 6300 m a.s.l.) in the year 1999 in a joint expedition of the Swiss Paul Scherrer Institut (PSI) and the French Institut de Recherche pour le Développement (IRD) using an electromechanical 7.6 cm diameter drill. Both ice cores reached bedrock at 138.7 and 136.7 m, respectively. The Tl record and the records of major ions described in this study are from the 138.7 m core. In the comparison between the continuous and the conventional

* Corresponding author e-mail: kellerhals@climate.unibe.ch, now at: Physics Institute, University of Bern, Switzerland.
† Department of Chemistry and Biochemistry, University of Bern.
‡ Paul Scherrer Institut.
§ Institute for Particle Physics.
∥ Oeschger Centre for Climate Change Research, University of Bern.

method for the analysis of trace elements, sections from the Grenzgletscher ice core (45°55′N, 7°52′E, ~4200 m a.s.l., Monte Rosa massif, Switzerland (21)) were used.

Nevado Illimani is located in the eastern Bolivian Andes where precipitation is not restricted exclusively to the wet season, as the eastern slopes of the Andes also get some precipitation during the dry season (22). A mean annual net accumulation of 0.58 m water equivalent (weq.) (23) allowed for highly resolved records. Englacial temperatures between −7 °C in the firn part and −8.4 °C near bedrock ensured the preservation of the chemical records.

Materials. Rigorous precleaning procedures were applied to all materials involved in the ICP-SFMS analysis. Containers for the ice samples from the conventional analysis and for the trace element calibration standards (125 and 30 mL bottles, high-density polyethylene (HDPE)), autosampler vials (2 mL, poly styrol (PS)), and bottles for stock solutions (30 mL, fluorine ethylene polypropylene (FEP)) were washed three times with 0.3 M HNO₃, prepared from ultrapure nitric acid (Ultrex II, J.T. Baker), triple-rinsed with ultrapure water (18.2 MΩ cm quality), and dried in a class-100 laminar flow bench. Polypropylene (PP) filters (to be placed on the MH) were rinsed with ultrapure water, stored in ultrapure water, and rinsed again before use. Wrist-length PE gloves were worn throughout sample preparation and analysis. Sample vials utilized in the ion chromatography (IC) analyses were rinsed five times with ultrapure water, dried, and capped under a class-100 laminar flow bench.

Ice Core Cutting and Sample Preparation. The individual ice core sections (60−75 cm in length) were cut for the continuous analysis with ICP-SFMS and for the analysis of major ions with IC in a cold room (−20 °C). To this end, two parallel bars with ~2.2 × 2.2 cm cross sections were cut from the inner part of the ice core using a modified band saw with a Teflon coated saw guide and tabletop (21). The bars for the continuous analysis were decontaminated at the breaks by removing the outermost 3 mm of ice using a precleaned ceramic knife. There was no need to physically decontaminate the external sides due to the use of a MH decontamination system where only meltwater from the innermost part was used for analysis. Without touching the decontaminated breaks, the ice bar was placed in a Plexiglas tube. Two blank ice core sections (prepared from frozen ultrapure water) of a length of ~10 cm were placed in front and at the end of the ice bar. The parallel ice bar dedicated to the analysis of major ions was cut into subsamples of a length of 2−3 cm, which were filled directly into precleaned IC vials and stored without acidification in a freezer until analysis.

The ice samples for the conventional trace element analysis were prepared according to established methods for the mechanical decontamination (19, 24). Ice core segments from the Grenzgletscher were cut to pieces of a maximum length of 30 cm. Such a piece was fixed in a Plexiglas holder in a class-100 clean bench in the cold room and decontaminated with precleaned stainless steel scalpels. Three consecutive layers were chiseled off, cleaning sample holder and scalpels from ice shavings between every step. PE gloves where worn throughout sample preparation and replaced after every step. The decontaminated piece was split into individual samples of a length of 7−9 cm which were directly filled into sample containers. Prior to analysis, the ice was melted and acidified to 0.3 M HNO₃ with ultrapure nitric acid under class-100 laminar flow benches. Aliquots were subsequently spiked with ^{103}Rh as internal standard and analyzed with ICP-SFMS.

Continuous Ice Melting (CIM) Device. The setup for the continuous analysis of trace elements in ice consists of two parts, (i) the melter system, and (ii) its coupling to the ICP-SFMS (Figure 1). The melter system was described in detail in Knüsel et al. (16) and features a perfluoralkoxy (PFA)-
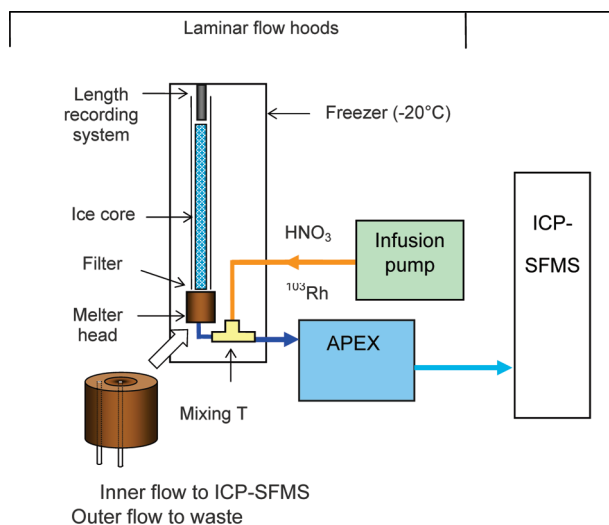

FIGURE 1. Design of the modified setup for the coupling of the continuous ice melting (CIM) device to the ICP-SFMS. Blue lines indicate the meltwater flow from the melter head via a mixing tee, where concentrated nitric acid and ^{103}Rh are added from an infusion pump (orange lines) to the Apex sample introduction system. From here, the analytes are transported as a dry aerosol to the inlet of the ICP-SFMS via Tygon tubing (light blue line). The melter head is located in an upright freezer at −20 °C. Melting device, Apex, infusion pump, and inlet of the ICP-SFMS are placed beneath class-100 laminar flow hoods. Scheme modified after Knüsel et al. (16).

coated aluminum MH mounted in an upright freezer (−20 °C). With three built-in 100 W cartridges, a temperature sensor, and a temperature controller, the MH is maintained at a temperature of 55 °C.

Right on the MH, the meltwater is split into two channels, physically separated by a ridge encircling the drain of the inner channel. The decontamination of the ice bar is performed directly on the MH by separating the meltwater of the potentially contaminated outer part from the meltwater of the innermost clean part of the core, which is used for analysis. To prevent clogging of the capillaries by insoluble dust particles, a PP filter (45 μm pore size) was placed on the MH and exchanged after every ice core section. A MH temperature of 55 °C resulted in an ice melting speed of 0.7−0.8 cm min^{-1}. To ensure a sufficient contact pressure of the ice bar on the MH, a weight of ~160 g was placed on top of the ice bar and a length recording system logged the progress of the melting process.

Coupling to the ICP-SFMS. The coupling of the continuous ice melting (CIM) device to the ICP-SFMS was facilitated with the integration of an APEX Q sample introduction system (Elemental Scientific Inc.). The meltwater from the inner drain of the MH was connected to the microflow PFA nebulizer of the APEX, operating in self-aspiration mode. After desolvation in the APEX, the analytes were transported as a dry aerosol to the inlet of the ICP-SFMS through Tygon tubing (Figure 1). Because of this setup, it was possible to acidify the meltwater to 0.3 M HNO₃ right after the MH and to reduce the length of the tubing where the analytes were transported as a liquid sample. This helped to minimize losses to the capillary walls and reduced potential memory effects.

ICP-SFMS Analyses. The trace element analyses were performed with an Element1 (Finnigan MAT). The APEX sample introduction system increased instrument sensitivity and reduced oxide formation in the plasma. The ICP-SFMS was calibrated daily with six standards bracketing the expected concentrations of trace elements in the ice. ^{103}Rh was used as internal standard to correct for plasma fluctuations in the conventional analysis. In the continuous analy-
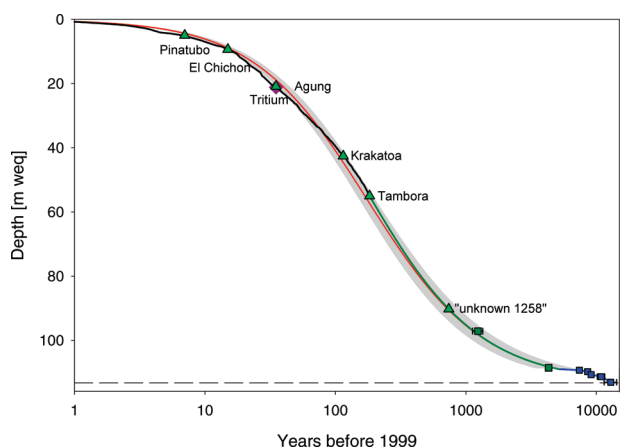
FIGURE 2. Depth-age relationship for the Illimani ice core. Different dating approaches were adopted: (i) Annual layer counting (black line) from 1999 A.D. to 1815 A.D. using seasonally varying ammonium concentrations and constraints from five previously identified volcanic horizons (Pinatubo 1991 A.D., El Chichón 1983 A.D., Agung 1963 A.D., Krakatoa 1883 A.D., and Tambora 1815 A.D., years of deposition were assumed to start 1 year after the eruption) (*23*). Volcanic eruption horizons are indicated by green triangles. The tritium horizon (assigned to 1964 A.D.) is given as additional time marker (purple diamond). (ii) Two-parameter model derived depth-age relationship (red line) using the volcanic eruption horizons (including the unknown 1258 A.D. horizon) and two calibrated ^{14}C ages (dark-green squares with 1σ ranges, 1σ ranges partly hidden beneath symbols). The 95% confidence band of the two-parameter model is indicated by the gray shading. To match the Tambora horizon, the model was shifted by 14.6 years (dark-green line). (iii) Linear interpolation (blue line) between calibrated ^{14}C ages (blue squares with 1σ ranges, 1σ ranges partly hidden beneath symbols). The bottom of the ice core is indicated with the dashed horizontal line.

sis, however, no normalization to an internal standard was performed, as it was observed that the variability in the internal standard, introduced by its addition via an infusion pump, was uncorrelated to the plasma fluctuations. Because of the difficulties that impeded the production of homogenously mixed frozen multielement ice standards to be used as calibration standards on the MH, an external calibration with liquid calibration standards was performed. Calibration correlation coefficients were generally higher than 0.999. In the continuous analysis, five consecutive scans were averaged to one data point, representing about 1 cm. Procedural blank concentrations were determined prior to the analysis of each ice core section by analyzing an identically prepared artificial ice bar of ~10 cm length. Every ice core section was then corrected by its individual procedural blank. The average procedural Tl blank level was 0.11 ± 0.10 pg g^{-1} ($n = 90$). Operating parameters for the continuous analysis with ICP-SFMS are given in part S1 of the Supporting Information.

IC Analyses. Major ions (F$^-$, HCOO$^-$, CH$_3$SO$_3^-$, Cl$^-$, SO$_4^{2-}$, C$_2$O$_4^{2-}$, NO$_3^-$, Na$^+$, NH$_4^+$, K$^+$, Mg^{2+}, Ca^{2+}) were analyzed using standard ion chromatography. Ultrapure water blanks were subtracted from the samples and for concentrations below detection limit (0.13 μg/L for F$^-$ and 1.2 μg/L for sulfate) a value of half of the detection limit was inserted.

Dating of the Ice Core. For the establishment of the Illimani time scale (Figure 2) a multiparameter approach was applied. From the glacier surface to 56.26 m weq. depth (corresponding to 1999−1809 A.D.), annual layer counting (ALC) was performed on the seasonally varying signals of ammonium and dust related species. The reference horizons from the tritium activity maximum (attributed to the year 1964 A.D.) and from a suite of volcanic eruptions (Pinatubo 1991 A.D., El Chichón 1983 A.D., Agung 1963 A.D., Krakatoa
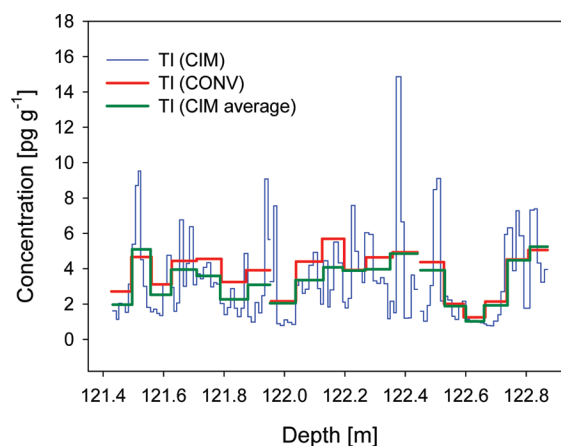

FIGURE 3. Records of Tl obtained with the continuous method for trace element analysis in ice (CIM, blue, resolution ~1 cm) and the conventional method (CONV, red, resolution 7−9 cm). For better comparison, the CIM values were averaged over the length of the conventional samples (CIM average, green). The ice used for this analysis was from the Grenzgletscher core and covered the time period 1937−1939 A.D. (*21*).

1883 A.D., and Tambora 1815 A.D.), which were identified in Knüsel et al. (*23*), served as fixed anchor points for the ALC (years of deposition were assumed to start one year after the eruption). The time scale was confirmed for the most recent 100 years by independent ^{210}Pb dating (*23*).

For the part of the core between 56.26 and 109 m weq. (corresponding to 1809 A.D. to ~5000 B.P.), a continuous depth-age relationship was obtained from a two-parameter model (*25*) that was applied to the five above-mentioned volcanic horizons, a further volcanic horizon from the massive "unknown 1258" eruption (*26*) and two calibrated ^{14}C time markers obtained with a radiocarbon dating method using microgram amounts of carbonaceous particles in ice (*27−29*). In this part, the depth−age relationship was revised compared to the dating by Knüsel et al. (*23*) due to the reassignment of the unknown 1258 eruption. This eruption had previously been ascribed to an electrical conductivity peak at 99.9 m weq. depth, but it could not be corroborated by the chemical signature at this depth. The exceptionally strong signals in exSO$_4^{2-}$ (nongypsum sulfate, calculated in microequivalent/L to exSO$_4^{2-}$ = SO$_4^{2-}$ − Ca^{2+}) and F$^-$ at 90.2 m weq. depth led to the reattribution of the unknown 1258 eruption to this horizon (*30*). Below 109 m weq., the core was dated by linear interpolation between additional six ^{14}C dates (*29*). Thus, the oldest ice of the Illimani ice core dates back ~13 000 years. The time scale covered by this study, however, only spans the last ~2000 years.

Results and Discussion

Accuracy of the Continuous Method. Currently no frozen standard reference material for trace elements in ice is available. We analyzed Tl in the riverine water reference material SLRS-4 from the National Research Council Canada, although there is no certified value for Tl in this or any other relevant water reference material. However, the Tl concentration of 6.7 ± 0.2 ng/l ($n = 8$) we found agrees very well with the preferred value (6.8 ± 1.3 ng/l) for Tl from the GeoReM database (*31*) of the Max Planck Institute for Chemistry in Mainz (Germany). To assess the accuracy of the continuous method for ice samples, a comparison to the well-established conventional method for trace element analysis in ice (*3, 18, 32, 33*) was performed. Results from this analysis are presented in Figure 3.

The close agreement between these two completely independent methods demonstrates that Tl can be accurately analyzed with the continuous method, providing a signifi-
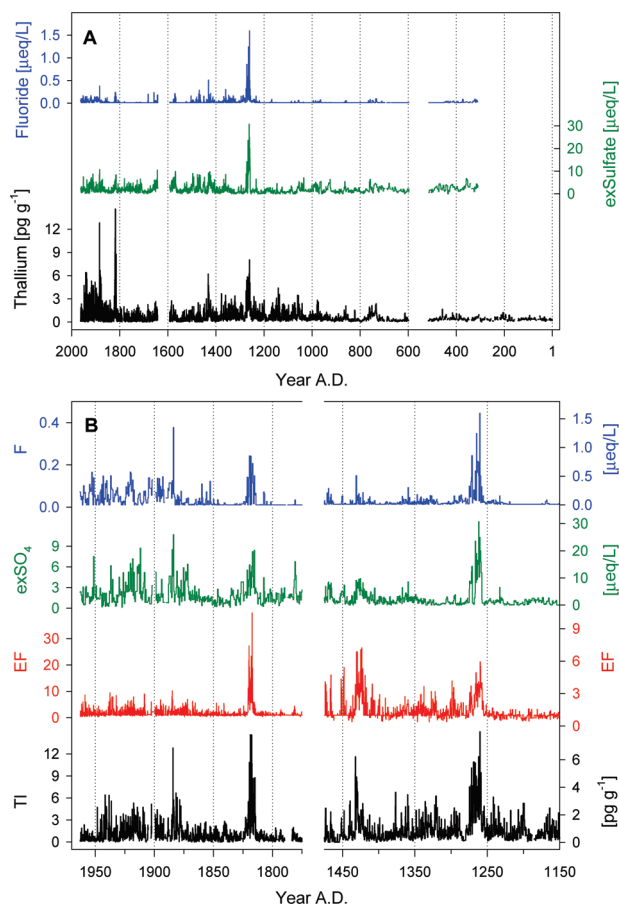
FIGURE 4. (A) Concentration records from the Illimani ice core for thallium (black) for the time period 1963−1 A.D. as well as for exSO$_4^{2-}$ (green) and F$^-$ (blue) for the time period 1963−310 A.D. Gaps in the records are due to sections of poor core quality where no measurements could be performed. The two time periods A.D. 1963−1750 and 1475−1150 are expanded in panel (B), displaying four volcanic signals from the unknown 1258, Kuwae, Tambora, and Krakatoa eruption (text) that are evident in the records of Tl concentrations (black), Tl enrichment factors (EF) (red), exSO$_4^{2-}$ concentrations (green), and F$^-$ concentrations (blue). Note the different scales (left and right) for the two different time periods.

cantly higher resolved record. High resolution is especially important in the lower parts of ice cores, where strong layer thinning leads to annual layer thicknesses of only a few centimeters. Because the samples for the continuous and the conventional method are not absolutely identical as they stem from parallel ice core sections, small variations between these parallel sections due to inhomogeneities in the ice or tilted layering cannot be excluded.

Thallium as a Volcanic Eruption Tracer. The continuous high-resolution Tl record covering the time period from 1963 A.D. to ~1 A.D. is presented in part A of Figure 4, along with records of F$^-$ and exSO$_4^{2-}$. In order to prevent that the records were biased by sporadic dust spikes, 23 clearly visible dust horizons were excluded from the analysis. In the resulting record, four prominent Tl concentration peaks stand out at ~1260, ~1430, 1816, and 1884 A.D. We propose that they represent signals from the massive explosive eruptions of the unknown 1258 volcano, of Kuwae (~1450 A.D.), Tambora (1815 A.D.), and Krakatoa (1883 A.D.). The average Tl concentration and EF in the record (volcanic eruption horizons excluded) is 0.60 pg g^{-1} and 1.24, respectively.

It is important to note that the time scale for the annual layer counted portion of the ice core back until 1809 A.D. was anchored to the volcanic eruption horizons described

above. Because these horizons were identified as peaks in the electrical conductivity measurement (ECM) by Knüsel et al. (23) prior to the analyses of major ions and trace elements, the volcanic anchor years were independently fixed to their corresponding depths by the ECM signal. The horizon with the exceptionally high concentrations in exSO$_4^{2-}$ and F$^-$, however, was assigned ex post to the massive unknown 1258 eruption (26) that is recorded in many ice cores. This attribution seems justified by both the excellent agreement with the two-parameter model that includes volcanic horizons as well as ^{14}C-dating points (Figure 2) and the counting of annual layers based on the ECM signal. Eight independent counting attempts yielded an approximate calendar year of 1271 A.D. ± 31 years (1σ) for the volcanic horizon.

The Tl signal at 1260 A.D. (part B of Figure 4) is characterized by an at least 3-fold increase in concentration, enrichment factors (EF) of up to 6, and accompanied by the highest concentrations in exSO$_4^{2-}$ and F$^-$ of the entire record. The EF for Tl relative to the Earth's crust were calculated as: EF Tl = ([Tl]/[U])$_{ice core}$/([Tl]/[U])$_{Earth's crust}$, where the values for Tl and U in the Earth's continental crust (0.52 and 1.7 μg g^{-1}, respectively) were taken from Wedepohl (9). EFs are used in this study to distinguish volcanic Tl horizons from dust layers. U was chosen as reference element because its concentrations in ice cores were shown to be dust derived for preindustrial time periods (34) and because it was the analysis of ^{238}U shortly after ^{205}Tl in the sequential mass scans of the ICP-SFMS that only allowed for an exact coregistration. The very high correlation between U and Sc, which is commonly used to calculate crustal EFs, supports our use of U as reference element (part S2 of the Supporting Information).

Tl concentrations and EF in the ~1430 A.D. signal are of comparable magnitude as in the unknown 1258 eruption event; the exSO$_4^{2-}$ and F$^-$ concentrations however are not as pronounced. It is noteworthy that the F$^-$ concentrations relative to Tl are different for the different eruptions. This indicates that certain past eruptions (e.g., 1430 A.D.) seem to have had different amounts of F$^-$ in their emissions or that F$^-$ was differently affected during transport and deposition.

Initial evidence for a major volcanic eruption in the A.D. 1450s came from ice cores from Antarctica (35). Subsequent research has detected the Kuwae eruption in ice cores from Antarctica and Greenland and concluded that it was one of the largest historical eruptions (36, 37). The offset of 20 years between the Tl signal in the Illimani ice core and the Kuwae 1450 A.D. eruption is well within the dating uncertainty for this time period, which is estimated from the two-parameter model to ± ~90 years and from the ECM signal layer counting to ± ~40 years (2σ values) for the year 1450 A.D.

The Tambora signal at 1816 A.D. shows both high Tl concentrations and EF of up to 30. The volcanic character of this horizon is corroborated by high exSO$_4^{2-}$ and F$^-$ concentrations (part B of Figure 4) as well as by a pronounced peak in the ECM signal (23). The Krakatoa eruption is recorded in the Illimani ice core as sharp peak in the Tl, exSO$_4^{2-}$, and F$^-$ concentrations of the year 1884 A.D., and the EF of ~10 during this event are second only to the Tambora eruption. However, the EF do not stand out when compared to the more recent values of first half of the 20th century. Together with the increase in Tl concentrations starting in the middle of the 19th century, this suggests that an anthropogenic contribution is discernible for the industrial time period. McConnell and Edwards (14) identified coal burning as the dominant source for Tl in a Greenland ice core during the coal-dominated early industrial era (1860−1940 A.D.). In the preindustrial part of the Illimani record, the EFs are close to unity, indicating that the background Tl mainly originated from rock and soil dust, with the excep-

tion of the volcanic events, when EF were distinctly higher. Our finding that Tl can serve as a tracer for volcanic emissions in preindustrial time periods is in agreement with the conclusion from McConnell and Edwards (*14*) that early sources for the Tl in their Greenland ice core were mainly volcanic emissions and continental dust.

It is interesting to note that other trace elements expected in volcanic layers as Pb, Cd, and Bi are not enriched above their crustal content in the ice sections with prominent Tl concentration peaks. In the case of Pb the anthropogenic input started around 1600 A.D., which cannot be corrected for with the concept of crustal enrichment factors. Sb and As could not be analyzed satisfactorily with our setup.

It has long been realized that the atmospheric load and deposition of geochemically rare trace metals cannot be accounted for by inputs of soil dust and sea salt alone (*38*). Tl and other ordinarily rare metals (Cd, Cu, In, Pb) were measured to be very abundant in plumes of quiescently degassing volcanoes (*39*). More recently it was proposed that the worldwide atmospheric metal injection by quiescently degassing volcanoes can account for the deposition of trace metals into preindustrial Antarctic ice (*5*). Furthermore, it was established that trace metals are also enriched in plumes of explosive volcanoes (*40*). Volcanic heavy metals are emitted from the magma in gaseous form, probably mainly as metal halides. Their high volatility favors the enrichment of these elements in volcanic gases compared to the composition of the magma (*41*). Hot, explosive eruptions can inject large quantities of volcanic gases into the stratosphere, where they have relatively long residence times due to slower removal processes. Through meridional circulations, the stratospheric volcanic aerosols can be dispersed over the whole globe within 1−2 years, but volcanic material from tropical eruptions generally remains enhanced in the tropics. Our finding that Tl, exSO$_4^{2-}$, and F$^-$ are highly correlated in the volcanic horizons suggests a joint stratospheric transport mechanism.

To conclude, the highly resolved Tl record that was obtained with an improved setup for the continuous analysis of trace elements in ice enabled the identification of short-term Tl peaks which were attributed to massive volcanic eruptions. We suggest that Tl can be used as a tracer for volcanic eruptions because it is enriched in volcanic sulfate aerosols that are known to be transported in the stratosphere over long distances. The fact that Tl is less susceptible to contamination than for example Cu, Zn, and Pb may make it an especially valuable volcanic tracer but further studies of volcanic horizons from low-latitude and polar ice cores are needed to explore its full potential.

Acknowledgments

Supporting Information Available

Additional tables and figures. This material is available free of charge via the Internet at http://pubs.acs.org.

Literature Cited

(1) Barbante, C.; Schwikowski, M.; Döring, T.; Gäggeler, H. W.; Schotterer, U.; Tobler, L.; Van De Velde, K.; Ferrari, C.; Cozzi, G.; Turetta, A.; Rosman, K.; Bolshov, M.; Capodaglio, G.; Cescon, P.; Boutron, C. Historical record of European emissions of heavy metals to the atmosphere since the 1650s from Alpine snow/ice cores drilled near Monte Rosa. *Environ. Sci. Technol.* **2004**, *38*, 4085–4090.

(2) Schwikowski, M.; Barbante, C.; Döring, T.; Gäggeler, H. W.; Boutron, C.; Schotterer, U.; Tobler, L.; Van De Velde, K. V.; Ferrari, C.; Cozzi, G.; Rosman, K.; Cescon, P. Post-17th-century changes of European lead emissions recorded in high-altitude alpine snow and ice. *Environ. Sci. Technol.* **2004**, *38*, 957–964.

(3) Barbante, C.; Veysseyre, A.; Ferrari, C.; Van de Velde, K.; Morel, C.; Capodaglio, G.; Cescon, P.; Scarponi, G.; Boutron, C. Greenland snow evidence of large scale atmospheric contamination for platinum, palladium, and rhodium. *Environ. Sci. Technol.* **2001**, *35*, 835–839.

(4) Gabrielli, P.; Barbante, C.; Boutron, C.; Cozzi, G.; Gaspari, V.; Planchon, F.; Ferrari, C.; Turetta, C.; Hong, S. M.; Cescon, P. Variations in atmospheric trace elements in Dome C (East Antarctica) ice over the last two climatic cycles. *Atmos. Environ.* **2005**, *39*, 6420–6429.

(5) Matsumoto, A.; Hinkley, T. K. Trace metal suites in Antarctic pre-industrial ice are consistent with emissions from quiescent degassing of volcanoes worldwide. *Earth Planet Sci. Lett.* **2001**, *186*, 33–43.

(6) Nriagu, J. O. A global assessment of natural sources of atmospheric trace metals. *Nature* **1989**, *338*, 47–49.

(7) Hinkley, T. K.; Lamothe, P. J.; Wilson, S. A.; Finnegan, D. L.; Gerlach, T. M. Metal emissions from Kilauea, and a suggested revision of the estimated worldwide metal output by quiescent degassing of volcanoes. *Earth Planet Sci. Lett.* **1999**, *170*, 315–325.

(8) Ferrari, C. P.; Hong, S.; Van de Velde, K.; Boutron, C. F.; Rudniev, S. N.; Bolshov, M.; Chisholm, W.; Rosman, K. J. R. Natural and anthropogenic bismuth in central Greenland. *Atmos. Environ.* **2000**, *34*, 941–948.

(9) Wedepohl, K. H. The composition of the continental crust. *Geochim. Cosmochim. Acta* **1995**, *59*, 1217–1232.

(10) *History, Production, and Uses of Thallium*; Nriagu, J. O., Ed.John Wiley and Sons: New York, 1998; p 1−14.

(11) Pacyna, J. M.; Pacyna, E. G. An assessment of global and regional emissions of trace metals to the atmosphere from anthropogenic sources worldwide. *Environ. Rev.* **2001**, *9*, 269–298.

(12) Cheam, V.; Lawson, G.; Lechner, J.; Desrosiers, R. Recent metal pollution in Agassiz Ice Cap. *Environ. Sci. Technol.* **1998**, *32*, 3974–3979.

(13) Krachler, M.; Zheng, J. C.; Fisher, D.; Shotyk, W. Atmospheric inputs of Ag and Tl to the Arctic: Comparison of a high resolution snow pit (AD 1994−2004) with a firn (AD 1860−1996) and an ice core (previous 16,000 yr). *Sci. Total Environ.* **2008**, *399*, 78–89.

(14) McConnell, J. R.; Edwards, R. Coal burning leaves toxic heavy metal legacy in the Arctic. *Proc. Natl. Acad. Sci. U.S.A.* **2008**, *105*, 12140–12144.

(15) Shotyk, W.; Krachler, M. Atmospheric deposition of silver and thallium since 12370 C-14 years BP recorded by a Swiss peat bog profile, and comparison with lead and cadmium. *J. Environ. Monit.* **2004**, *6*, 427–433.

(16) Knüsel, S.; Piguet, D. E.; Schwikowski, M.; Gäggeler, H. W. Accuracy of continuous ice-core trace-element analysis by inductively coupled plasma sector field mass spectrometry. *Environ. Sci. Technol.* **2003**, *37*, 2267–2273.

(17) McConnell, J. R.; Lamorey, G. W.; Lambert, S. W.; Taylor, K. C. Continuous ice-core chemical analyses using inductively coupled plasma mass spectrometry. *Environ. Sci. Technol.* **2002**, *36*, 7–11.

(18) Barbante, C.; Cozzi, G.; Capodaglio, G.; van de Velde, K.; Ferrari, C.; Boutron, C.; Cescon, P. Trace element determination in alpine snow and ice by double focusing inductively coupled plasma mass spectrometry with microconcentric nebulization. *J. Anal. At. Spectrom.* **1999**, *14*, 1433–1438.

(19) Candelone, J. P.; Hong, S.; Boutron, C. F. An improved method for decontaminating polar snow or ice cores for heavy-metal analysis. *Anal. Chim. Acta* **1994**, *299*, 9–16.

(20) Krachler, M.; Zheng, J.; Fisher, D.; Shotyk, W. Analytical procedures for improved trace element detection limits in polar ice from Arctic Canada using ICP-SMS. *Anal. Chim. Acta* **2005**, *530*, 291–298.

(21) Eichler, A.; Schwikowski, M.; Gäggeler, H. W.; Furrer, V.; Synal, H. A.; Beer, J.; Saurer, M.; Funk, M. Glaciochemical dating of an ice core from upper Grenzgletscher (4200 m a.s.l.). *J. Glaciol.* **2000**, *46*, 507–515.

(22) Garreaud, R. D.; Vuille, M.; Clement, A. C. The climate of the Altiplano: Observed current conditions and mechanisms of past

changes. *Palaeogeogr. Palaeoclimatol. Palaeoecol.* **2003**, *194*, 5–22.

(23) Knüsel, S.; Ginot, P.; Schotterer, U.; Schwikowski, M.; Gäggeler, H. W.; Francou, B.; Petit, J. R.; Simões, J. C.; Taupin, J. D. Dating of two nearby ice cores from the Illimani, Bolivia. *J. Geophys. Res.* **2003**, *108*, 4181.

(24) Boutron, C. F.; Batifol, F. M. Assessing laboratory procedures for the decontamination of polar snow or ice samples for the analysis of toxic metals and metalloids. *Ann. Glaciol.* **1985**, *7*, 7–11.

(25) Thompson, L. G.; Mosley-Thompson, E.; Davis, M. E.; Bolzan, J. F.; Dai, J.; Klein, L.; Gundestrup, N.; Yao, T.; Wu, X.; Xie, Z. Glacial stage ice-core records from the subtropical Dunde Ice Cap, China. *Ann. Glaciol.* **1990**, *14*, 288–297.

(26) Stothers, R. B. Climatic and demographic consequences of the massive volcanic eruption of 1258. *Clim. Change* **2000**, *45*, 361–374.

(27) Jenk, T. M.; Szidat, S.; Schwikowski, M.; Gäggeler, H. W.; Wacker, L.; Synal, H. A.; Saurer, M. Microgram level radiocarbon (^{14}C) determination on carbonaceous particles in ice. *Nucl. Instrum. Methods Phys. Res., Sect. B* **2007**, *259*, 518–525.

(28) Ruff, M.; Wacker, L.; Gäggeler, H. W.; Suter, M.; Synal, H. A.; Szidat, S. A gas ion source for radiocarbon measurements at 200 kV. *Radiocarbon* **2007**, *49*, 307–314.

(29) Sigl, M.; Jenk, T. M.; Kellerhals, T.; Szidat, S.; Gäggeler, H. W.; Wacker, L.; Synal, H. A.; Boutron, C.; Barbante, C.; Schwikowski, M. Towards radiocarbon dating of ice cores. *J. Glaciol.* In press.

(30) Kellerhals, T.; Brütsch, S.; Sigl, M.; Knüsel, S.; Gäggeler, H. W.; Schwikowski, M. Ammonium concentration in ice cores–a new proxy for regional temperature reconstruction? Submitted.

(31) GeoRem database. http://georem.mpch-mainz.gwdg.de/.

(32) Planchon, F. A. M.; Boutron, C. F.; Barbante, C.; Wolff, E. W.; Cozzi, G.; Gaspari, V.; Ferrari, C. P.; Cescon, P. Ultrasensitive determination of heavy metals at the sub-picogram per gram level in ultraclean Antarctic snow samples by inductively coupled plasma sector field mass spectrometry. *Anal. Chim. Acta* **2001**, *450*, 193–205.

(33) Gabrielli, P.; Barbante, C.; Turetta, C.; Marteel, A.; Boutron, C.; Cozzi, G.; Cairns, W.; Ferrari, C.; Cescon, P. Direct determination of rare earth elements at the subpicogram per gram level in antarctic ice by ICP-SFMS using a desolvation system. *Anal. Chem.* **2006**, *78*, 1883–1889.

(34) Barbante, C.; Van De Velde, K.; Cozzi, G.; Capodaglio, G.; Cescon, P.; Planchon, F.; Hong, S.; Ferrari, C.; Boutron, C. Post-World War II uranium changes in dated Mont Blanc ice and snow. *Environ. Sci. Technol.* **2001**, *35*, 4026–4030.

(35) Delmas, R. J.; Kirchner, S.; Palais, J. M.; Petit, J. R. 1000 years of explosive volcanism recorded at the South Pole. *Tellus B* **1992**, *44*, 335–350.

(36) Cole Dai, J. H.; Mosley Thompson, E.; Wight, S. P.; Thompson, L. G. A 4100-year record of explosive volcanism from an East Antarctica ice core. *J. Geophys. Res.* **2000**, *105*, 24431–24441.

(37) Zielinski, G. A.; Mayewski, P.; Meeker, L. D.; Whitlow, S.; Twickler, M.; Morrison, M. C.; Meese, D. A.; Gow, A. J.; Alley, R. Record of volcanism since 7000 B.C. from the GISP2 Greenland ice core and implications for the volcano-climate system. *Science* **1994**, *264*, 948–952.

(38) Patterson, C. C.; Settle, D. M. Magnitude of lead flux to the atmosphere from volcanoes. *Geochim. Cosmochim. Acta* **1987**, *51*, 675–681.

(39) Hinkley, T. K.; Lecloarec, M. F.; Lambert, G. Fractionation of families of major, minor, and trace metals across the melt-vapor interface in volcanic exhalations. *Geochim. Cosmochim. Acta* **1994**, *58*, 3255–3263.

(40) Lepel, E. A.; Stefansson, K. M.; Zoller, W. H. Enrichment of volatile elements in the atmosphere by volcanic activity: Augustine volcano 1976. *J. Geophys. Res.* **1978**, *83*, 6213–6220.

(41) Symonds, R. B.; Rose, W. I.; Reed, M. H.; Lichte, F. E.; Finnegan, D. L. Volatilization, transport and sublimation of metallic and non-metallic elements in high temperature gases at Merapi Volcano, Indonesia. *Geochim. Cosmochim. Acta* **1987**, *51*, 2083–2101.

ES902492N